A nature-derived, flexible and three dimensional (3D) nano-composite for chronic wounds pH monitoring

Manni Yang, Kwang-leong Choy*

Institute for Materials Discovery, Faculty of Mathematical & Physical Sciences, University College London, 107 Roberts Building, Malet Place, London, WC1E 7JE, UK

*Corresponding author: k.choy@ucl.ac.uk

Abstract

Current technologies on conductive carbon aerogels are merely for application of super-capacitors, anodes of lithium ion batteries and electrocatalysts. To our best knowledge, carbon nanofibre (CNF) aerogels in biomedical application of chronic wound monitoring have not been reported yet. In this paper, we proposed a chronic wounds pH sensor, which is based on 3D free-standing conductive CNF aerogel derived from pyrolyzed bacterial cellulose (p-BC) as conducting substrate and it is incorporated with flexible and proton-selective PDMS/PANI composite. The resulted p-BC/PDMS/PANI nanocomposite is soft, flexible, and can exhibit near Nernst limit pH sensitivity (~-50.4 mV/pH) in pH buffer solution, and -29 mV/pH in *in vitro* simulated wound fluid. This renders its applications in flexible bio-sensors and smart wound dressings.

Introduction

Unlike acute wounds which will heal in a short term, chronic wounds require extensive therapy and healing monitoring process due to bacterial infections. For chronic wounds, pH is a key indicative parameter in wound monitoring, for change of pH is often caused by bacteria infections. The pH value

in chronic wounds is often higher than 7.4, due to the alkaline by-products produced in the process of bacterial proliferation[1,2], while the healthy skin is slightly acid with pH 5.5-6.5[3]. In order to promptly and effectively treat wound areas, pH is measured at different locations in wound area, however, chronic wounds are in need of multiple measurements throughout the wound with high spatial resolutions which is beyond the capacity of most commercial probe. Recent flexible pH sensors often require complicated manufacturing method and expensive materials.

Bacterial cellulose (BC), a nanomaterial mainly produced by *Acetobacter xylinus*, is a highly crystalline linear polymer of glucose[4]and has 3D nano-network interconnected nano-fibres, with diameters of 20-100 nm[5]. Taking advantages of unique structure of BC, pyrolyzed BC (p-BC) has been used as precursor materials for carbon nano-fibres in applications of stretchable conductors[6], super-capacitors[7,8], and lithium ion battery anode[9,10]. The major advantages of using p-BC are the easy fabrication, low-industrial cost and mechanical robust 3D carbon nano-network structures.

In this paper, we demonstrated pyrolyzed BC/ polydimethylsiloxane (PDMS)/polyaniline (PANI) (p-BC/PDMS/PANI) nanocomposite as 3D flexible pH sensor used in chronic wounds with near-Nernst pH sensitivity.

Experiment materials and methods

Materials

BC pellicles were grown by *Acetobacter xylinum* (JCM 10150, Sigma-Aldrich, UK), obtained from University of Westminster, London, UK. Sylgard 184 silicone elastomer base and curing agent were purchased from Dow Corning (Midland, MI, USA). Polyaniline in emeraldine base (EB) (Mw~100,000), hydrochloride acid (37%, Mw~36.46), cyclohexane (99.5%, Mw~84.16), sodium hydroxide (97%, Mw~40), phosphate buffer saline (PBS)(0.1M, pH 7.4), and human serum (type AB) were purchased from Sigma (Sigma-Aldrich, UK). pH buffer solutions were purchased from Fisher Scientific (Fisher scientific Ltd, UK).

Methods

The BC pellicles were first cut into rectangular shapes (30*20*1 mm) with a sharp blade, frozen in freezer (-15^{o}C)and then freeze-dried in a bulk tray dryer at a sublimating temperature of –48 ^{o}C and a pressure of 0.04 mbar. The obtained BC aerogels were then pyrolyzed under flowing argon at 600–800^{o}C to generate p-BC aerogels. PANI ink was prepared according to procedures in publication by Pooria et.al [11] where PANI (EB) were doped with HCl acid to form PANI in emeraldine salt (ES). PDMS (10:1 curing ratio) was diluted using cyclohexane solution (50 wt.% in H_2O) at a weight ratio 1:1 and mixed with the prepared PANI ink. The p-BC/PDMS/PANI nanocomposite was fabricated by infiltrating the p-BC aerogel into PDMS/PANI ink followed by degassing in a vacuum oven and curing at 75^{o}C for 2 h. Characterizations are listed in the supplementary information.

Results & Discussions

Structural characterizations

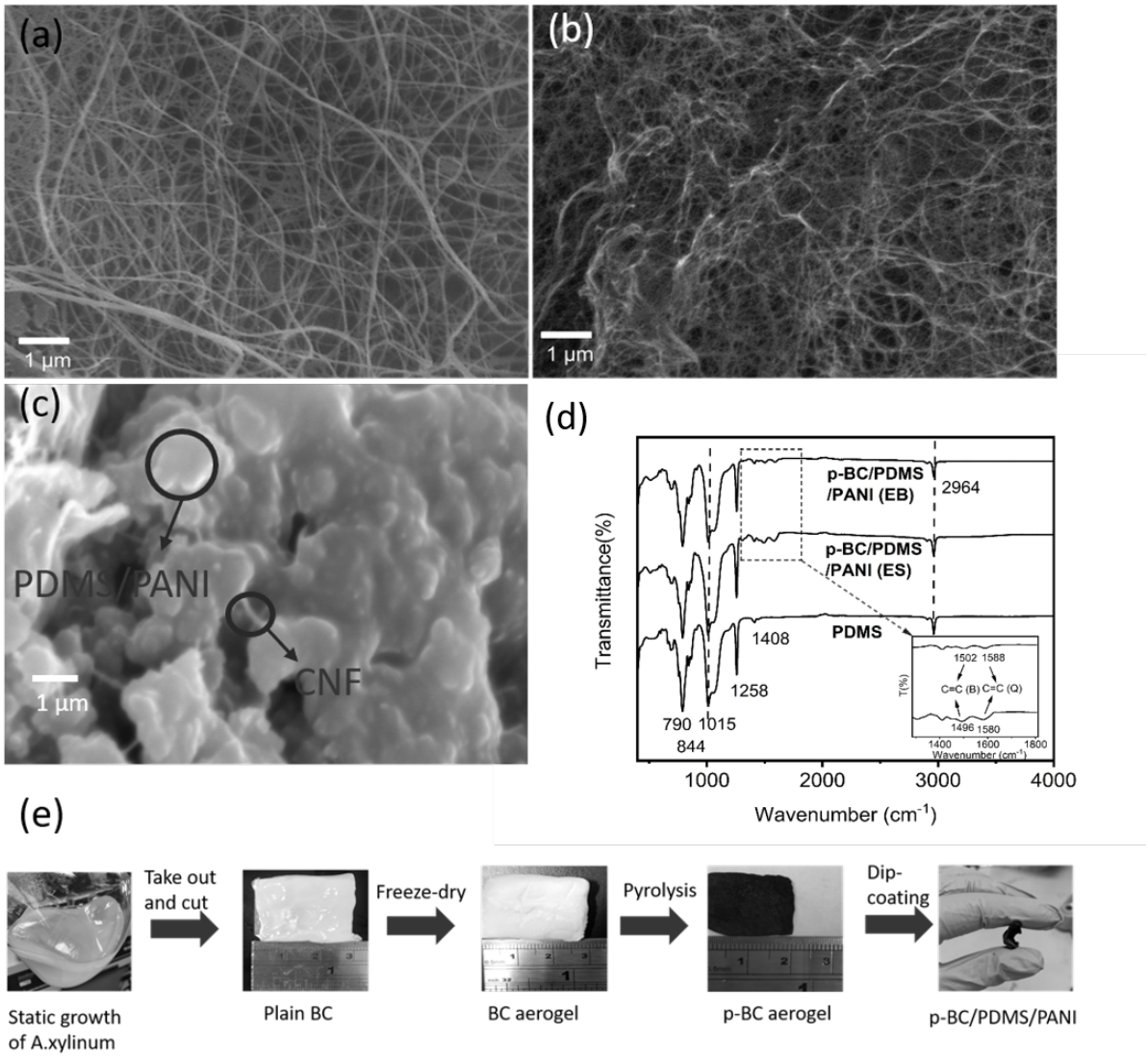

Figure 1. SEM images of (a) plain BC, (b) pyrolyzed BC aerogel, and (c) p-BC/PDMS/PANI aerogel; (d) FTIR characterizations of p-BC/PDMS/PANI (EB and ES) and PDMS; (e) Fabrication process of p-BC/PDMS/PANI nanocomposite.

As SEM images show in figure 1, BC has 3D nano-network structure with interconnected nanofibres, p-BC has remained 3D nano-network for 3D carbon nano-fibre network structure, which can induce the electrons to move fast, as well as high surface area for PANI/PDMS to be coated. In addition, diluted PDMS has used to maintain nano-porous structure, which is beneficial for protonation of PANI

conducting in pH sensing. In order to verify p-BC/PDMS/PANI sample, Figure 1. (d) shows the FTIR spectroscopy of p-BC/PDMS/PANI as compared with p-BC/PDMS doped with PANI (EB), and PDMS. The peaks are slightly shifted from 1588 to 1580 cm^{-1} and 1502 to 1496 cm^{-1}, which are assigned to the C=C stretching of the quinoid ring and benzenoid ring, respectively, indicating PANI (EB) [12] turned into PANI (ES) [13]. In addition, the peak intensity of 1496 cm^{-1} is stronger than 1502 cm^{-1}, further confirming the presence of PANI (ES)[14]. The bands at 1408 and 1258 cm^{-1} indicate asymmetric and symmetrical deformations of C-H in $Si(CH_3)_2$ group, and the peak at 1015 cm^{-1} could be assigned to Si-O, confirming PDMS infiltration[15,16]. The peaks at 844 and 790 cm^{-1} suggest the deformation of C-H and Si-C bond stretching in PDMS[17]. Figure 1.(e) illustrates the fabrication process of p-BC/PDMS/PANI nanocomposite. Porosity and pore sizes analysed by BET (SI. Table 1) reveal that both types of BC aerogels have ultra large surface area, nano-scale pore sizes and relatively small pore volume, which is beneficial for acting as a conductive substrate of pH sensor.

Electrical characterizations and pH sensing test

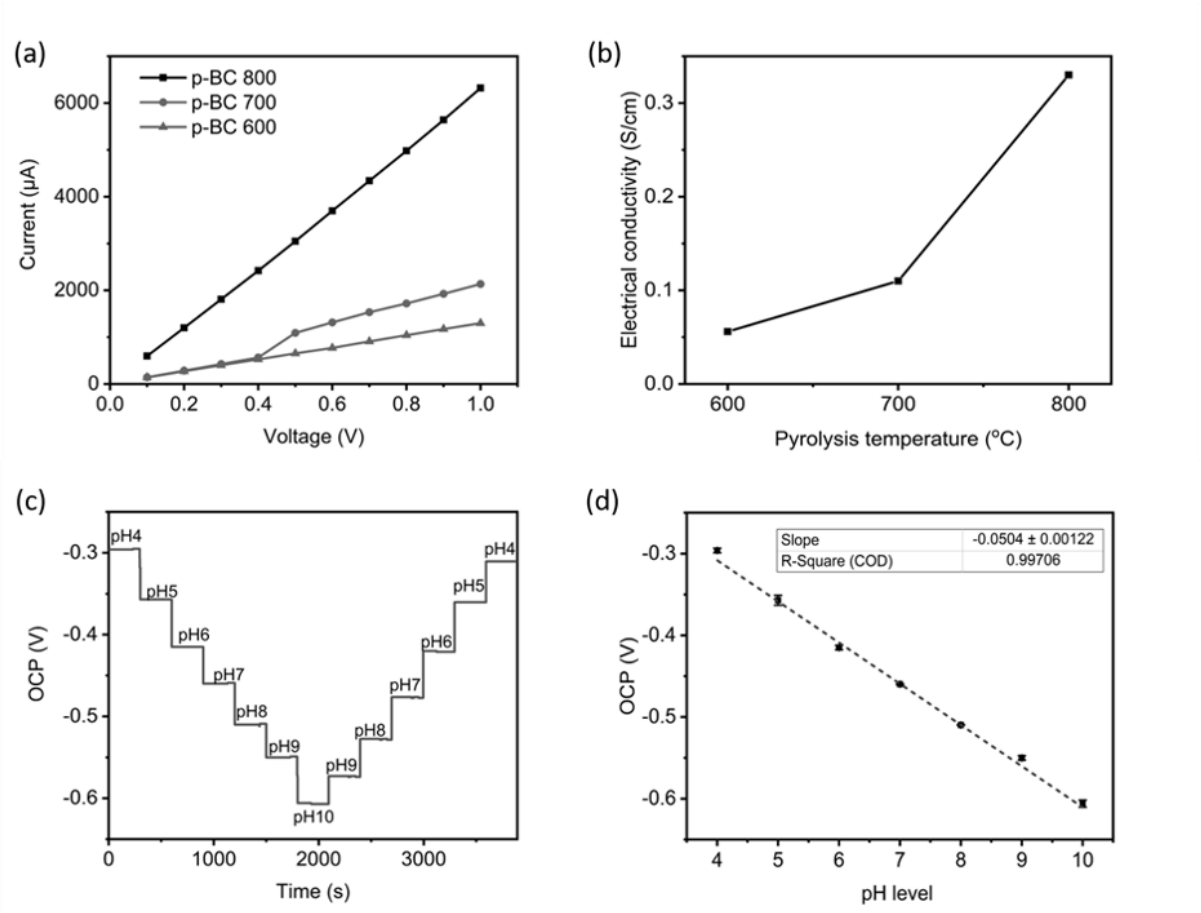

Figure 2. Electrical characterizations of p-BC/PDMS/PANI nanocomposite: (a) the electrical conductivity test of BC aerogel pyrolyzed under 600°C- 800°C, (b) the calculated electrical conductivity of p-BC pyrolyzed at 600, 700 or 800°C, (c) open circuit potential (OCP) test for p-BC/PDMS/PANI nanocomposite pH sensor in response to pH levels ranging from 4 to 10, (d) the measured sensor response to various pH levels between 4 and 10.

The conductivity test in Figure 2 (a) and (b) shows the p-BC had increased conductivity with increased pyrolyzed temperature, and both p-BC/PDMS and p-BC have similar tendency of conductivity even when pyrolyzed at temperature under 800°C. In addition, p-BC with higher pyrolyzed temperature reveals higher output current thus higher conductivity. The Figure 2 (c) and (d) show the sensor response for increasing and decreasing pH levels where there are great changes in output potential. It is indicated that the proposed p-BC/PDMS/PANI nano-composite has experienced steady pH sensitivity lasting for 5 min and the open-circuit potential has decreased with increased pH level. The linear reduction has

indicated pH sensitivity as -50.4 mV/pH with coefficient of determination R^2 as 0.997, which is near-Nernst limit. It also indicates that acidic solutions enabled more protonation occurred in PANI.

***In vitro* pH sensing test**

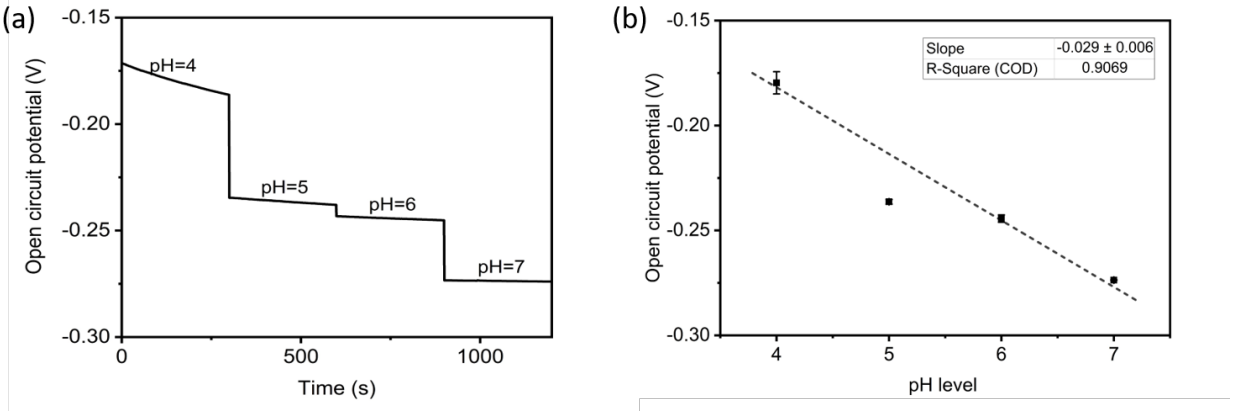

Figure 3. *In vitro* pH sensitivity test for open-circuit potential by placing fabricated samples into different pH solutions against (a) measuring time, (b) pH level.

In order to simulate wound exudate to the maximum extent, *in vitro* pH sensing test was also performed for our sensor by incorporating human serum into PBS buffer solutions, which was reported to have a chemical environment similar to the wound healing tissues[18]. Figure 3 (a) indicates similar response of the sensor tested in commercial pH buffer solutions. The potentiometric response as a function of pH level in Figure 3 (b) shows an average linear relationship between 4 to 7, with sensitivity of -29 mV/pH and R^2 is 0.9. In addition, the *in vitro* test did not apply to higher pH level above 7 due to the inconspicuous changes in OCP value as compared with the acidic environment. The results indicate the protonation can be affected by the high serum protein load that is able to bind to a lot of protons and this is becoming more obvious in alkaline. In this case, further experiments can be done in sensor optimization.

Conclusions

In this paper, a nature-derived, cost-effective, and flexible 3D pH sensor was developed for use in chronic wounds monitoring. Based on the naturally derived carbon aerogel, the developed fabrication process is simple and relatively greener as compared with PANI sensors made by electrochemical deposition methods. The sensor performance was tested in both commercial pH buffer solutions and *in vitro* wound simulated fluid, which showed a linear potential and sensitivity of -50.4 mV/pH and -29 mV/pH, with stable response in different pH levels. The p-BC/PDMS/PANI nanocomposite showed a great potential for integration with low-cost wound dressings in chronic wounds monitoring.

Acknowledgements

The author would like to thank Professor Ipsita Roy and her group members in University of Westminster who kindly provided the BC bacteria strain and training.

REFERENCES

[1] L.A. Schneider, A. Korber, S. Grabbe, J. Dissemond, Influence of pH on wound-healing: a new perspective for wound-therapy?, Arch. Dermatol. Res. 298 (2007) 413–420. https://doi.org/10.1007/s00403-006-0713-x.

[2] S. Schreml, R.J. Meier, O.S. Wolfbeis, M. Landthaler, R.-M. Szeimies, P. Babilas, 2D luminescence imaging of pH in vivo, Proc. Natl. Acad. Sci. 108 (2011) 2432–2437. https://doi.org/10.1073/pnas.1006945108.

[3] M. Ochoa, R. Rahimi, B. Ziaie, Flexible sensors for chronic wound management, IEEE Rev. Biomed. Eng. 7 (2014) 73–86. https://doi.org/10.1109/RBME.2013.2295817.

[4] A.F. Jozala, L.C. De Lencastre-novaes, A.M. Lopes, V.D.C. Santos-ebinuma, P.G. Mazzola, A. Pessoa-jr, Bacterial nanocellulose production and application : a 10-year overview, Appl Microbiol Biotechnol. 100 (2016) 2063–2072. https://doi.org/10.1007/s00253-015-7243-4.

[5] L.R. Lynd, P.J. Weimer, W.H. Van Zyl, I.S. Pretorius, Microbial Cellulose Utilization : Fundamentals and Biotechnology, Microbiol. Mol. Biol. Rev. 66 (2002) 506–577. https://doi.org/10.1128/MMBR.66.3.506.

[6] H.W. Liang, Q.F. Guan, Z.Z. Zhu, L.T. Song, H. Bin Yao, X. Lei, S.H. Yu, Highly conductive

and stretchable conductors fabricated from bacterial cellulose, NPG Asia Mater. 4 (2012) e19-6. https://doi.org/10.1038/am.2012.34.

[7] D.T.L. Feili Lai, Dr Yue-E Miao, Lizeng zuo, Youfang Zhang, Carbon Aerogels Derived from Bacterial Cellulose/Polyimide Composites as Versatile Adsorbents and Supercapacitor Electrodes, ChemNanoMat. 2 (2016) 212–219.

[8] X. Wang, D. Kong, Y. Zhang, B. Wang, X. Li, T. Qiu, Q. Song, J. Ning, Y. Song, L. Zhi, All-biomaterial supercapacitor derived from bacterial cellulose, Nanoscale. 8 (2016) 9146–9150. https://doi.org/10.1039/c6nr01485b.

[9] B. Wang, X. Li, B. Luo, J. Yang, X. Wang, Q. Song, S. Chen, L. Zhi, Pyrolyzed bacterial cellulose: A versatile support for lithium ion battery anode materials, Small. 9 (2013) 2399–2404. https://doi.org/10.1002/smll.201300692.

[10] H. Yang, Y. Li, P. Long, J. Han, C. Cao, F. Yao, W. Feng, Amorphous red phosphorus incorporated with pyrolyzed bacterial cellulose as a free-standing anode for high-performance lithium ion batteries, RSC Adv. 8 (2018) 17325–17333. https://doi.org/10.1039/c8ra02370k.

[11] P. Mostafalu, M. Akbari, K.A. Alberti, Q. Xu, A. Khademhosseini, S.R. Sonkusale, A toolkit of thread-based microfluidics, sensors, and electronics for 3D tissue embedding for medical diagnostics, Microsystems Nanoeng. 2 (2016) 16039. https://doi.org/10.1038/micronano.2016.39.

[12] M. Ibrahim, E. Koglin, Spectroscopic study of polyaniline emeraldine base: Modelling approach, Acta Chim. Slov. 52 (2005) 159–163.

[13] P. Srinivasan, R. Gottam, Infrared Spectra: Useful Technique to Identify the Conductivity Level of Emeraldine form of Polyaniline and Indication of Conductivity Measurement either Two or Four Probe Technique, Mater. Sci. Res. India. 15 (2018) 209–217. https://doi.org/10.13005/msri/150302.

[14] H. Noby, A.H. El-Shazly, M.F. Elkady, M. Ohshima, Novel preparation of self-assembled HCl-doped polyaniline nanotubes using compressed CO2-assisted polymerization, Polymer (Guildf). 156 (2018) 71–75. https://doi.org/10.1016/j.polymer.2018.09.060.

[15] A. Mata, A.J. Fleischman, S. Roy, Characterization of polydimethylsiloxane (PDMS) properties for biomedical micro/nanosystems., Biomed. Microdevices. 7 (2005) 281–293. https://doi.org/10.1007/s10544-005-6070-2.

[16] F.A.B. Silva, F.A. Chagas-Silva, F.H. Florenzano, F.L. Pissetti, Poly(dimethylsiloxane) and poly[vinyltrimethoxysilane-co-2-(dimethylamino) ethyl methacrylate] based cross-linked oroganic-inorganic hybrid adsorbent for copper(II) removal from aqueous solutions, J. Braz. Chem. Soc. 27 (2016) 2181–2191. https://doi.org/10.5935/0103-5053.20160110.

[17] F.L. Pissetti, I.V.P. Yoshida, Y. Gushikem, Y. V. Kholin, Metal ions adsorption from ethanol solutions on ethylenediamine-modified poly(dimethylsiloxane) elastomeric network, Colloids Surfaces A Physicochem. Eng. Asp. 328 (2008) 21–27. https://doi.org/10.1016/j.colsurfa.2008.06.016.

[18] N.J. Trengove, S.R. Langton, M.C. Stacey, Biochemical analysis of wound fluid from nonhealing and healing chronic leg ulcers, Wound Repair Regen. 4 (1996) 234–239. https://doi.org/10.1046/j.1524-475X.1996.40211.x.